The SNAI2-ELF3-AS1 Feedback Loop Drives Gastric Cancer Metastasis and Regulates ELF3 Expression At Transcriptional and Post-Transcriptional Levels

Dandan Li
Hubei University of Medicine
Li Shen
Hubei University of Medicine
Mengjie Xu
Hubei University of Medicine
Xudong Zhang
Hubei University of Medicine
Zhen Chen
Hubei University of Medicine
Pan Huang
Hubei University of Medicine
Congcong Huang
Hubei University of Medicine
Shanshan Qin (qinss77@163.com)
Hubei University of Medicine https://orcid.org/0000-0002-8527-5278

Research Article

Keywords: ELF3-AS1, SNAI2 overexpression, transcriptional regulation, mRNA stability, gastric cancer metastasis

Posted Date: October 19th, 2021

DOI: https://doi.org/10.21203/rs.3.rs-880315/v1

Abstract

Background

The reason for continued overexpression of SNAI2 in tumor metastasis remains largely unclear. The oncogene SNAI2 promotes tumor metastasis by regulating the expression of downstream target genes. In theory, these target genes should include not only protein-coding genes or miRNAs, but also lncRNAs. However, no lncRNA has been reported to be regulated by SNAI2 to date.

Methods

RNA-seq, CHIP and dual-luciferase reporter assay were performed to identify lncRNAs regulated by SNAI2. MicroRNA-seq and RNA-seq studies were conducted to reveal the biological function of ELF3-AS1 in GC. RNA pulldown and CHIRP assays were conducted to identify the protein that interacts with ELF3-AS1.

Results

In this study, the lncRNAs that regulated by SNAI2 were identified in gastric cancer (GC) by RNA sequencing. The ELF3 gene and its antisense lncRNA ELF3-AS1 were both transcriptionally repressed by SNAI2 or SNAI1. Down-regulation of ELF3-AS1 and ELF3 predicted poor prognosis in GC. Nuclear localized lncRNA ELF3-AS1 negatively regulated GC cell cycle progression via suppressing G1/S transition and histone synthesis. ELF3-AS1 mainly inhibited GC metastasis by repressing SNAI2 signaling. Additionally, ELF3-AS1 modulated ELF3 mRNA stability by RNA-RNA interaction. The RNA duplexes formed by ELF3 mRNA and lncRNA ELF3-AS1 directly interacted with NF45/NF90 complex. In turn, the NF45/NF90 complex dynamically regulated the expression of ELF3-AS1 and ELF3 by affecting the stability of the RNA duplex.

Conclusions

The double-negative feedback loop SNAI2-ELF3-AS1 drives GC metastasis by continuously activating SNAI2 signaling and regulates the expression of epithelial tumor suppressor ELF3 at transcriptional and post-transcriptional levels.

Background

Gastric cancer (GC) is the third most common cause of cancer-related deaths.(1, 2) Though current treatments for GC patients have been greatly improved, the 5-years overall survival rate remains unsatisfactory to date due to the inconvenience of early diagnosis of GC.(3) Metastasis is the leading cause of cancer-related deaths worldwide.(4) Therefore, it is urgently necessary to unravel the molecular mechanisms underlying metastasis.

The transcription repressor SNAI2 (also known as SLUG), which belongs to the SNAIL transcription factor family, is known to be one of the master regulators of epithelial–mesenchymal transition (EMT).(5)

Accumulating evidence have shown that SNAI2 is widely overexpressed in tumors and promotes tumor metastasis by transcriptionally regulating downstream target genes, especially the EMT-related genes.(6, 7) However, the reason for the sustained overexpression of SNAI2 during tumor metastasis remains largely unclear.

Long non-coding RNAs (lncRNAs) are a group of classic endogenous non-coding RNAs with a length of more than 200 nucleotides.(8) Increasing studies have shown that lncRNA dysregulation plays broad and complex roles in tumorigenesis and metastasis.(9) Transcription is the first and most heavily regulated step in gene expression.(10) Like protein-coding genes and microRNAs, the expression of lncRNAs is also regulated by corresponding transcription factors. Thus, the abnormal expression of transcription factors usually results in the aberrant expression of downstream lncRNAs, coding-genes and miRNAs. For examples, Li et al. reported that the down-regulation of the transcription factor ELF3 leads to lncRNA UBE2CP3 overexpression in GC.(11) Liu et al. reported that lncRNA HNF1A-AS1 overexpression was due to the activated transcription by transcription factor EGR1.(12)

In this study, we identified a novel antisense lncRNA ELF3-AS1, which was strongly repressed by SNAI2. The SNAI2-repressed lncRNA ELF3-AS1 negatively regulates SNAI2 signaling pathway in GC. Our finding highlights that SNAI2 and ELF3-AS1 form a double-negative feedback loop to maintain SNAI2 overexpression, thereby driving GC metastasis. To our knowledge, the work present here represents the first data on the biological function of lncRNA ELF3-AS1 in GC. Our finding provides a new and somewhat surprising explanation that SNAI2 can achieve self-overexpression by modulating downstream lncRNAs.

Materials And Methods

Cell transfection and establishment of cell lines

Human gastric cancer cell lines AGS, NCL-N87, MGC803 and HGC-27 were purchased from GeneChem (Shanghai, China). The human gastric cancer cell lines (BGC823, SGC7901 and MKN45) and the normal gastric cell line GES-1 were purchased from the Shanghai Cell Bank of Chinese Academy of Sciences. The siRNAs listed in Table S1 were designed and synthesized by Genepharma (Shanghai, China). Briefly, GC cell lines were seeded into 6-well plates and grown overnight. The next day, when the cell plating density reached 20%-30%, GC cells were transfected with siRNAs (final concentration, 50 nM) by Lipofectamine 2000 (Invitrogen) according to the manufacturer's instructions. The lentiviruses for knockdown of ELF3-AS1 in GC cell lines were purchased from Genepharma (Shanghai, China). The lentiviruses for overexpression of SNAI1 and SNAI2 in GC cell lines were purchased from GeneChem (Shanghai, China). Transfection was performed according to the manufacturer's instructions. At the indicated time points, the cells were harvested for mRNA and protein analysis as well as for other assays.

Clinical GC samples

The study protocol was approved by the Human Research Ethics Committee of Hubei University of Medicine (2018-TH-035). The procedures were in accordance with the Helsinki Decaration of 1975.

Written informed consent was obtained from all patients. Tissue samples were immediately frozen in liquid nitrogen after resection and stored at − 80°C until use. All samples were pathologically confirmed.

RNA sequencing

The total RNA in GC cells was extracted to perform RNA sequencing (RNA-seq). A total amount of 1.5 μg RNA per sample was used as input material for the RNA sample preparations. The whole step of library construction and sequencing was performed at Shanghai Lifegenes Technology Co., Ltd. The RNA-seq data was uploaded on the GEO section of NCBI web server. The GEO accession numbers were GSE161551 (SNAI2/SNAI1 overexpression), GSE161291 (ELF3-AS1 knockdown) and GSE161544 (ILF2/ILF3 knockdown).

MicroRNA sequencing analysis

After effectively knocked down ELF3-AS1 expression in GC cells, the total RNA of each sample was extracted and then sent to BGI company (Wuhan, China) for microRNA purification and miRNA sequencing analysis. The normalized expression level of each microRNA was calculated by TPM value. The Log2FC value was calculated to estimate between-group differences. For each microRNA, if the fold change is more than 1, the difference between negative control and the matched target samples is set to be significant. The microRNA-seq data was uploaded on the GEO section of NCBI web server. The gene expression omnibus accession number is GSE161553.

Mouse xenograft model

Four-week-old female BALB/c nude mice were purchased from the Laboratory Animal Center of Hubei University of Medicine and maintained in a temperature-controlled (21°C) and light-controlled pathogen-free animal facility with free access to food and water. All animals were treated in accordance with guidelines of the Committee on Animals of the Hubei University of Medicine. 5×10^6 of SGC7901 cells (shNC and shELF3-AS1#2) were injected into subcutaneous tissue of female BALB/c nude mice. After 28 days, all the mice were sacrificed, and the tumors were collected for weighing and volume measurement. The tumor volume was calculated using the following formula: volume = length × $(\text{width})^2/2$. The study protocol was approved by the Experimental Animal Research Ethics Committee of Hubei University of Medicine (2019-056).

RNA Fish assay

Briefly, GC cell lines were seeded and fixed with 4% paraformaldehyde. The next day, when the cell plating density reached 50%-70%, GC cells were treated with 0.5% Triton followed by pre-hybridization. Overnight hybridization was performed with a 10 mM probe concentration. The RNA FISH kit was purchased from RiboBio company (Guangzhou, China). The experiment was performed according to the manufacturer's instructions. The 5'FAM-ELF3-AS1 probes were designed and synthesized by Sangon Biotech (Shanghai). Images were taken with a confocal microscope (Zeiss).

Chromatin immunoprecipitation assay

Chromatin immunoprecipitation (CHIP) assays were performed using CHIP Assay Kit (56383S, Cell Signal Technology, USA) according to the manufacturer's protocol. Briefly, the SGC7901 cell line were collected and fixed for 10 min at 37 with 1% formaldehyde, followed in sequence with SDS lysis and DNA shearing, protein and DNA immunoprecipitation, cross-linked DNA reversal and DNA purification, and finally the immunoprecipitated DNA fragments were detected by PCR assays. The normal rabbit IgG was used as the negative control. The primers for CHIP were listed in Table S1.

Western blot assay

Gastric cancer cells were lysed in RIPA buffer added 1 mM PMSF. Approximately 100 μg of total protein was electrophoresed through 10% SDS polyacrylamide gels and were then transferred to a PVDF membrane. After blocking with 5% skimmed milk at 4°C for 1h, the membrane was incubated with primary antibody at 4°C overnights. The blots were then washed and incubated with horseradish peroxidase (HRP)-conjugated secondary antibody (1: 10000, Earthox) for 1.5 h at room temperature. Detection was performed by using a SuperLumia ECL HRP Substrate Kit (Abbkine) and visualized using a Bio-Rad Imaging System (USA). The detail information of antibodies used in this study was listed in the Table S2.

RNA Immunoprecipitation assay

After crosslinking with 0.5% formaldehyde for 10 min at room temperature, cells were harvested and lysed in RIP lysis buffer with RNasin (1000 U/ml), DNase I (50 U/ml) and protease inhibitor cocktail. After the genomic DNA was digested, lysates were further subjected to sonication. Supernatants cleared by centrifugation were incubated with the anti-ILF3 antibody (Proteintech, China) or IgG overnight at 4°C. Protein A/G beads were added for a further 4 h incubation at room temperature. After the beads were washed, immunocomplexes of proteins and RNAs were de-crosslinked at 95°C for 15 min. The immunoprecipitated RNAs were then purified for RNA sequencing and qRT-PCR analysis.

RNA pull-down assay

Briefly, 831bp length of sense and antisense ELF3-AS1 sequences were cloned into pGEM-T Easy (Promega). In vitro transcription was carried out and RNA was purified and labeled with Biotin at 3' end. Cells were harvested and resuspended in freshly prepared lysis buffer supplemented with 50 U/mL RNase inhibitor (Takara) and a protease/phosphatase inhibitor cocktail (Roche). Sense and antisense RNAs were captured on magnetic beads (Pierce) and were incubated with cell lysates in protein-RNA-binding buffer (Thermo Scientific) overnight at 4°C with agitation. RNA-binding protein complexes were washed five times with ice-cold wash buffer and were boiled in SDS lysis buffer for western blot assay and mass spectrometry (MS) analysis.

Chromatin isolation by RNA purification (CHIRP) assay

Briefly, the CHIRP assay was carried out to verify the interaction between ELF3-AS1 and RNA binding proteins. A 3' end Biotin modified-DNA probe targeting ELF3-AS1 was designed and synthesized by Sangon. Before crosslinking, SGC7901 cells were grown and seeded into 10 cm dishes. Cell lysates were

harvested after incubation of 48 h with a confluence of 60–80%. Cells were cross-linked with 1% formaldehyde and sonicated for the hybridization reaction. After the chromatin was sheared into 100–500 bp fragments, the cell lysates were incubated with the biotinylated DNA probe solution for 4h at 37°C. The binding complex was covered with streptavidin-conjugated magnet beads. The proteins were finally eluted and purified from the magnet beads for real-time qPCR or mass spectrometry and western blotting analyses.

Statistical analysis

For gene expression analysis of different subtypes of GC, the P values were estimated using Mann–Whitney nonparametric test. Survival curves were calculated using the Kaplan–Meier method, and differences between the curves were analysed using the log-rank test. All the rest of the experiments were used unpaired *t*-test or one-way ANOVA test. For all experiments, a minimum of triplicates per group and repetition of at least three times was applied to achieve reproducibility. All tests with p values less than 0.05 considered statistically significant.

Other methodologies are detailed in the Supplementary information.

Results

Exploration of lncRNAs regulated by transcription repressor SNAI2 in GC

To explore the lncRNAs regulated by SNAI2, RNA sequencing studies were conducted in the GC cell line overexpressing SNAI2. A total of 318 coding genes, 70 lncRNAs were strongly repressed by SNAI2, while 55 coding genes and 53 lncRNAs were greatly upregulated by SNAI2 (|Log2FC| >1, Table S3). As shown in the Fig. 1A, the expression of IGFBP1/3, ITGB4, CLDN1/4, TJP3, EFNA1, KRT80, ELF3 etc. were strongly repressed by SNAI2, while the expression of CYR61, CTGF, IL11, ID2/3, RBM3, THBS1 etc. were strongly upregulated by SNAI2. Similarly, around 123 lncRNAs, including linc01315, MIR210HG, FZD10-DT, linc00963, HOXB-AS3, LUCAT1, ITPR1-DT, PDCD4-AS1, ZNF197-AS1 etc., greatly altered their expression after overexpressing SNAI2 (|Log2FC| >1). Among them, ELF3-AS1 was one of the top 10 lncRNAs that strongly repressed by SNAI2 (Fig. 1B).

The biological function of lncRNA ELF3-AS1 remains largely unknown in cancers. To further confirm whether ELF3-AS1 could be negatively regulated by SNAI2, loss-of-function and gain-of-function studies regarding SNAI2 were further performed in two GC cell lines. The qPCR analysis showed that ELF3-AS1 and ELF3 were significantly downregulated in the SNAI2 overexpression cell lines but were significantly upregulated in the SNAI2-depletion cell lines (Fig. 1C-E). These results suggested that both ELF3-AS1 and ELF3 were negatively regulated by SNAI2 in GC.

ELF3-AS1 is an antisense lncRNA (head-to-head) of the epithelial tumor suppressor gene *ELF3*. Promoter analysis revealed that ELF3-AS1 promoter contained the sequence “GGTACAGGTGGGT”, which was

predicted to be recognized by both SNAI2 and SNAI1. This sequence was located 829bp upstream of the ELF3-AS1 transcription start point, which was also the junction point between exon 2 and intron 2 of the ELF3 gene (Fig. 1F). Thus, we speculated that both ELF3-AS1 and ELF3 might be transcriptionally regulated by SNAI2 and SNAI1.

ELF3-AS1 and ELF3 were transcriptionally repressed by both SNAI2 and SNAI1.

LncRNA ELF3-AS1 is abundant in human cells and can be effectively captured by magnetic beads when RNA sequencing. In order to make our results more convincing, we used RNA-seq studies to visualize the expression of ELF3-AS1 and ELF3. As expected, RNA-seq data showed that ELF3-AS1 and ELF3 transcripts were both greatly reduced in SNAI2 (or SNAI1) overexpression cell lines (Fig. 2A-F). Besides, the inhibitory intensity of SNAI2 on the expression of ELF3 and ELF3-AS1 was much greater than that of SNAI1 (Fig. 2B, E).

Furthermore, to figure out whether the negative regulation of ELF3 and ELF3-AS1 by SNAI2/SNAI1 occurred at the transcriptional level, dual-luciferase assays and CHIP assays were performed in the SNAI1 and SNAI2 overexpression cell lines. As shown in Fig. 2G, when the SNAI1/2 binding sequence was mutated, the strong repression of SNAI1/2 overexpression on luciferase expression could be partially restored, suggested that this sequence was necessary for SNAI1/SNAI2 to inhibit ELF3/ELF3-AS1 expression. On the other hand, CHIP assays showed that SNAI1 and SNAI2 could directly bind to the ELF3-AS1 promoter (Fig. 2H-J). Taken together, both SNAI2 and SNAI1 could transcriptionally repress the expression of ELF3 and ELF3-AS1 in GC.

The reduced ELF3-AS1 and ELF3 expression were clinically associated with poor prognosis in GC.

The ELF3-AS1 expression pattern in 30 pairs of GC tissues was determined by qPCR assay. As expected, ELF3-AS1 was down-regulated in more than 80% of GC samples compared to the corresponding normal samples (Figure. 3A). On the other hand, we analyzed the correlation between level of ELF3-AS1 expression and the clinical characteristics of GC tissues from the cancer genome atlas (TCGA, n = 375) database. LncRNA ELF3-AS1 was low expressed in diffuse and poorly differentiated gastric cancer tissues (Fig. 3B and C, $p < 0.0001$). However, no significant changes in ELF3-AS1 expression levels were observed between GC patients with different TNM stages (Fig. 3D-F, $p > 0.05$). Overall survival analysis showed that GC patients with lower expression level of ELF3-AS1 possessed shorter overall survival time (Fig. 3G, $p = 0.029$).

Our previously published study had implied that transcription factor ELF3 plays tumor-suppressive roles in GC.(11, 13) Herein, we further confirmed that ELF3 protein and ELF3 mRNA were significantly

downregulated in GC (Fig. 3H-J). Besides, lower expression of ELF3 was observed in the diffuse GC compared with intestinal GC (Fig. 3K). The low expression of ELF3 was positively correlated with the malignant progression of GC (Fig. 3L and M). Moreover, patients with lower ELF3 expression had a poorer overall survival time and disease-free survival time in the GSE62254 GC cohort (Fig. 3N and O).

According to the clinical outcomes, both ELF3-AS1 and ELF3 functioned as tumor suppressors in GC. Since ELF3-AS1 and ELF3 were transcriptionally repressed by SNAI2 and SNAI1, we further analyze the expression signatures and prognostic values of SNAI2 and SNAI1 in GC. As expected, SNAI2 and SNAI1 were upregulated in GC (Figure S1A and B). Besides, the overexpression of SNAI2 and SNAI1 predicted poor prognosis in the two independent GC cohorts (Figure S1C-F).

ELF3 negatively regulated GC cell metastasis but cannot regulate ELF3-AS1 expression

Protein coding genes are usually highly co-expressed with their neighboring lncRNAs(14). Similarly, ELF3-AS1 and ELF3 were confirmed to be highly co-expressed in the normal stomach tissues, GC cell lines and tissues (Fig. 4A-D, $p < 0.0001$). Interestingly, when the ELF3-AS1 was effectively knocked down in GC cell lines, the transcripts of ELF3 were significantly reduced to approximately 60–70% (Figure. 4E-H). However, it's not clear how ELF3-AS1 affects ELF3 expression in GC.

Given ELF3 belongs to ETS transcription factor family, we initially assumed that the co-expression of ELF3-AS1 and ELF3 may be due to ELF3 regulating the expression of ELF3-AS1. To verify this possibility, loss-of-function and gain-of-function studies regarding on ELF3 were performed in two GC cell lines. However, the expression of ELF3-AS1 had no significant alteration after knockdown or overexpressing of ELF3 in GC (Figure. 4I and J). Although transcription factor ELF3 cannot regulate ELF3-AS1 expression, the scratch wound healing assays and transwell assay still confirmed that ELF3 negatively regulated GC cell migration and invasion (Figure. 4K and L).

ELF3-AS1 mainly inhibited GC metastasis through repressing SNAI2 signaling

To determine whether ELF3-AS1 has a tumor-suppressive effect in GC, loss- and gain-of-function studies were performed in GC. Cell apoptosis assay showed that depletion of ELF3-AS1 remarkably accelerated early apoptosis of GC cells (Figure S2A). Besides, cell proliferation, transwell and scratch wound healing assays showed that ELF3-AS1 knockdown promotes GC cell proliferation, migration and invasion (Figure. S2B-F). The overexpression of ELF3-AS1 significantly inhibited the proliferation, migration and invasion ability of HGC-27 cells (Figure. S2G-I). Moreover, we examined the effect of ELF3-AS1 silencing in a xenograft GC model *in vivo*. The tumor growth of GC cells silencing ELF3-AS1 was significantly increased when compared to that of the control GC cells (Figure. S2J and K). These results together suggested that ELF3-AS1 inhibited proliferation and metastasis of GC cells *in vitro* and *in vivo*.

We analyzed the differentially expressed miRNAs after ELF3-AS1 knockdown by miRNA sequencing (Fig. 5A). Surprisingly, among the top 10 miRNAs that were most significantly down-regulated after ELF3-AS1 knockdown, miR-33a, miR-33b and miR-203a were reported to be able to target SNAI2 expression (Fig. 5B).(15–17) To confirm the reliability of miRNA sequencing, we examined the expression level of miR-33a, miR-33b and miR-203a in the ELF3-AS1 knockdown cell lines by qRT-PCR assays. The results showed that knockdown of ELF3-AS1 can indeed significantly down-regulate the expression of miR-33a, miR-33b and miR-203a (Fig. 5C-E). In turn, the depletion of ELF3-AS1 led to significant up-regulation of SNAI2 mRNA and protein (Fig. 5F-I).

In addition, the gene expression profiles of SNAI2 overexpression and ELF3-AS1 knockdown were very similar (Figure S3A). The genes strongly regulated by SNAI2 overexpression also have similar expression changes in ELF3-AS1-depleted GC cells (Figure S3B-D). For examples, the genes strongly inhibited by SNAI2 overexpression, such as IGFBP3, ITGB4, TJP3, PPL and DDIT4, were also significantly down-regulated in the ELF3-AS1-depleted GC cell lines. The genes strongly induced by SNAI2 overexpression, such as IL11, THBS1, INSL4 and linc02104, were also remarkably upregulated in the ELF3-AS1-depleted GC cell lines. These results strongly implied that knockdown of ELF3-AS1 could not only upregulate SNAI2 expression but also greatly activate the downstream signaling of SNAI2 in GC.

Based on above findings, we speculated ELF3-AS1 may inhibit GC progression through repressing SNAI2 expression. To verify this possibility, the rescue assays were performed in two different GC cell lines that stably knocked down ELF3-AS1. The results showed that exogenous siRNA targeting SNAI2 rescued the tumorigenic properties of ELF3-AS1-depleted GC cell lines (Fig. 5J and K). These data strongly indicated that ELF3-AS1 mainly inhibited the migration and invasion of GC cells through repressing SNAI2 signaling.

The nuclear-localized lncRNA ELF3-AS1 plays critical roles in the cell cycle progression.

The biological function of lncRNA is closely related to its subcellular location.(18) ELF3-AS1 was a nuclear-localized lncRNA in GC (Fig. 6A and B). Previous study had reported that ELF3-AS1 was a cell cycle-related lncRNA.(19) Our study also showed that lncRNA ELF3-AS1 played essential roles in cell cycle progression. Silencing ELF3-AS1 significantly accelerated the G1/S transition of the cell cycle in GC (Fig. 6C and D). Interestingly, RNA-seq analysis showed that knockdown of ELF3-AS1 resulted in a significant up-regulation of almost all histone-coding genes by more than 2 times (Figure. 6E and F). It's well known that the synthesis of histones is mainly in the S phase of cell cycle, which is synchronized with DNA replication. These results indicated that ELF3-AS1 negatively regulates cell cycle progression of GC cells by affecting G1/S transition and histone synthesis.

To better understand of the molecular mechanism of ELF3-AS1 in regulating the cell cycle process, we analyzed the expression changes of cell cycle-related genes after knockdown of ELF3-AS1. The results

showed that knockdown of ELF3-AS1 increased the expression of CDK6 and CASP7, while decreased the expression of CDKN1A (also known as p21) in GC (Figure. 6G and H). The p21 proteins functioned as a cell cycle checkpoint of G1/S transition.(20) The CDK6/CCND1 protein complex is very important for cell cycle G1 phase progression and G1/S transition.(21) Therefore, we considered that the promotion of G1/S transition caused by ELF3-AS1 knockdown may be due to the downregulation of P21 and the upregulation of CDK6.

ILF2/ILF3 complex could directly modulate the stability of ELF3-AS1/ELF3 RNA duplex.

The potential proteins interacted with lncRNA ELF3-AS1 were identified by RNA pull-down analysis (Fig. 7A). According to the mass spectrometry (MS) analysis of the differential bands located at 45 Daltons (Fig. 7B), there were 7 proteins with matching coverage greater than 20% (Table S4). 3 of them, RINI, ILF2 (also known as NF45) and TARBP2, were double-strand RNA binding proteins (Fig. 7C). Interestingly, another protein named ILF3 (also known as NF90/NF110) was also appear in the MS results of this band (Fig. 7D and E). Our subsequent western blot assay further verified that ILF2, ILF3 and TARBP2 could bind to exogenous lncRNA ELF3-AS1 (Fig. 7F). Moreover, CHIRP pulldown assay verified that endogenous ELF3-AS1 also bound to the ILF2 and ILF3 proteins (Fig. 7G and H). The Venn plot showed that approximately 22 proteins are displayed at the intersection of the three MS results, including ILF2, ILF3, RINI, etc. (Table S4-6, Fig. 7G and H). RNA immunoprecipitation assay showed that the ELF3-AS1 transcripts bound to ILF2 and ILF3 proteins were thousands of times higher than the control IgG group (Fig. 7I-K). To figure out which segment of ELF3-AS1 transcript could interact with ILF2 and ILF3, we truncated ELF3-AS1 transcripts of different lengths (Fig. 7L). The results showed that the first exon of ELF3-AS1 was necessary for the interaction between the ELF3-AS1 and the ILF2/ILF3 complex (Fig. 7M and N).

The *ELF3* gene has many different transcripts due to alternative splicing. Among those different types of ELF3 transcripts, ELF3-201, ELF3-202 and ELF3-203 can encode full-length ELF3 protein. It's worth mentioning that the ELF3-201 transcript and the ELF3-AS1 transcript overlapped by about 664 nucleotides (Fig. 8A). In other words, ELF3-AS1 can combine with the first exon region of ELF3-201 to form a double-stranded RNA molecule. On the other hand, RNA-seq analysis revealed that knockdown of ELF3-AS1 had a more profound effects on ELF3-201 expression compared to the ELF3-203 or any other ELF3 transcripts level (Fig. 8B). These data implied that the ILF2/ILF3 complex may bind to the double-stranded RNA formed by ELF3-AS1 and ELF3-201. To further verify this probability, we also examined the ELF3-201 transcript level in the RIP assays of ILF2/ILF3. The ELF3-201 transcripts bound to ILF2 and ILF3 were much higher than the control IgG group (Fig. 8C-E), suggesting ILF2/ILF3 complex could bind to the double-stranded RNA formed by the first exons of ELF3-AS1 and ELF3-201.

It has been reported that ILF2/ILF3 complex play roles in regulating mRNA stability.(22) The RNA-seq data and the qPCR assays indicated that knockdown of ILF3 significantly decreased the mRNA level of

ELF3-AS1 and ELF3-201, while knockdown of ILF2 significantly increased the mRNA level of ELF3-AS1 and ELF3-201 (Fig. 8F and G, Figure S4A-I). These results suggested that ILF2 and ILF3 protein possessed opposite effects on the stability of ELF3-AS1 transcripts. Previous study reported that NF45 functions as a regulatory subunit in ILF2/ILF3 complexes.(23) Interestingly, we also noted that knockdown of ILF2 could obviously affect the alternative splicing of ILF3 gene (Fig. 8H). qRT-PCR assays showed that knockdown of ILF2 significantly upregulate the expression of NF90, but significantly decreased the expression of NF110 (FigureS4J and K). Therefore, we speculated ILF2 (NF45) might regulate ELF3-AS1 and ELF3-201 expression through affecting the alternative splicing of ILF3 gene.

Discussion

EMT (Epithelial-Mesenchymal Transition) is a key factor leading to the poor prognosis of GC patients. Oh et al. previously reported that GC patients with mesenchymal phenotype has a poorer prognosis compared to the GC patients with epithelial phenotype.(24) Similarly, Cristescu et al. has reported that GC patients belongs to EMT subtypes possessed the worst prognosis.(25) SNAI2 (Slug), a master regulator of EMT, is usually overexpressed in tumor metastasis. As a transcription factor, SNAI2 exerts its biological functions by regulating downstream target genes, including protein-coding genes and non-coding RNAs.(26–28) However, no lncRNA has been reported to be regulated by SNAI2.

In this study, we took SNAI2 as a breakthrough point to screen lncRNAs regulated by SNAI2 in GC. Overexpression of SNAI2 caused a 2-fold change in the expression of about 123 lncRNAs (Table S3). ELF3-AS1 was one of the top 10 lncRNAs most significantly repressed by SNAI2 overexpression. Furthermore, ELF3-AS1 and ELF3 gene were both identified to be directly repressed by SNAI2 and SNAI1 at the transcriptional level. Though SNAI1 had a similar effect to SNAI2 in inhibiting the expression of ELF3 and ELF3-AS1 or any other downstream target genes, the regulatory efficient of SNAI1 on the expression of target genes is much weaker than that of SNAI2. This result indicates that SNAI2 may be the major effect gene in SNAI family transcription factors compared to SNAI1.

Why does SNAI2 transcriptionally repress the expression of lncRNA ELF3-AS1? SNAI2 is a rapid turnover protein.(29) Recently, Kang et al. had reported that SNAI2 protein turnover was regulated by the ubiquitin proteasome system (UPS).(5, 6) However, in theory, the regulation of SNAI2 protein turnover should be not only at the (post-) translational level, but also at the (post-) transcriptional level. Herein, our findings strongly indicated that the SNAI2-repressed lncRNA ELF3-AS1 played an essential role in maintaining SNAI2 mRNA stability. Knockdown of ELF3-AS1 results in decreased expression levels of miRNAs targeting SNAI2, upregulation of SNAI2 mRNA and protein, and activation of downstream signaling of SNAI2 (Figures. 5, S3). Additionally, analysis of the RNA-seq data from another independent study (GSE92250) also confirmed that ELF3-AS1 knockdown led to SNAI2 mRNA upregulation in the A549, Hela and Caki-2 cell lines (Figure S5), suggested the negative regulation of SNAI2 expression by ELF3-AS1 was widely in cancers.(19) Besides, the overall survival analysis based on the TCGA data showed that ELF3-AS1 and SNAI2 possessed opposite prognosis in pan-cancers (Figure S6). These findings highlight that SNAI2 achieve self-overexpression by transcriptionally repressing ELF3-AS1. Once SNAI2 is

overexpressed, it can transcriptionally repress ELF3-AS1 expression, thereby maintaining self-overexpression state in tumor metastasis (Fig. 8I).

ELF3 gene and its antisense lncRNA ELF3-AS1 were highly co-expressed in stomach and GC tissues. Our finding highlights that SNAI2-ELF3-AS1 feedback loop regulates ELF3 expression at transcriptional and post-transcriptional levels (Fig. 8I). At transcriptional level, ELF3-AS1 and ELF3 genes shared the same promoter, which makes them both under the regulation of transcription factors (such as SNAI2 and SNAI1). At the post-transcriptional level, lncRNA ELF3-AS1 could stabilize ELF3 mRNA by form RNA duplexes with the overlapping region of ELF3-201 mRNA. Besides, the ILF2/ILF3 complex could directly regulate mRNA stability of ELF3-AS1 and ELF3 via interacting with the RNA duplex formed by lncRNA ELF3-AS1 and ELF3 mRNA.

Antisense lncRNAs share sequence similarity with the corresponding parental genes but in the sense/antisense orientation, meaning they have the potential to interact with each other and to form RNA-RNA duplexes.(30) For examples, Jadaliha et al. had reported that natural antisense lncRNA PDCD4-AS1 regulates PDCD4 mRNA stability by formation of the RNA duplex PDCD4-AS1/PDCD4.(31) Similarly, Li et al. have reported that the antisense intronic lncRNA UBE2CP3 and IGFBP7 mRNA can form an RNA duplex, which could strengthen UBE2CP3 mRNA stability in GC.(11) Herein, we also found that the first exon of ELF3-AS1 could bind with the overlapping regions of the first exon of ELF3-201 transcripts to form double-stranded RNA molecules, which interacted with ILF2/ILF3 complex. However, whether the ILF2/ILF3 complex can regulate the SNAI2 signaling by regulating the stability of ELF3-AS1 transcripts remains to be further studied.

Conclusions

ELF3-AS1 is identified as a SNAI2-repressed lncRNA that inhibits GC metastasis through repressing SNAI2 signaling. The double-negative feedback loop SNAI2/ELF3-AS1 plays critical roles in driving GC metastasis via continuously activating SNAI2 signaling. LncRNA ELF3-AS1 and ELF3 mRNA can directly form RNA duplexes and interact with the NF45/NF90 complex. In turn, the NF45/NF90 complex can dynamically regulate the expression of ELF3-AS1 and ELF3 by affecting the stability of the RNA duplex. Our work presents the first evidence for the biological function of the lncRNA ELF3-AS1 in GC, which may help to better understand the over-activation of the SNAI2 signaling in tumor metastasis.

Abbreviations

GC: Gastric cancer

TCGA: The Cancer Genome Atlas

UTR: Untranslated region

EMT: epithelial mesenchymal transition

TPM: transcripts per million

qRT-PCR: quantitative reverse transcription Polymerase Chain Reaction

GEO: Gene Expression Omnibus

FPKM: Fragments Per Kilobase of exon model per Million mapped fragments

STAD: Stomach adenocarcinoma

HNSC: Head and Neck squamous cell carcinoma

KIRC: Kidney renal clear cell carcinoma

ESCA: Esophageal carcinoma

READ: Rectum adenocarcinoma

LIHC: Liver hepatocellular carcinoma

LUSC: Lung squamous cell carcinoma

CHIRP: Chromatin Isolation by RNA Purification

Declarations

Ethics approval and consent to participate

The study is approved by the Ethics Committee of Hubei University of Medicine (2018-TH-035). All participants provided written informed consent.

Consent for publication

All authors agreed on the manuscript.

Availability of data and materials

The datasets supporting the conclusions of this article are available in the GEO repository (GSE161291, GSE161553, GSE161551 and GSE161544).

To review GEO accession GSE161291:

Go to https://www.ncbi.nlm.nih.gov/geo/query/acc.cgi?acc=GSE161291

Enter token idqrumukbbytxer into the box

To review GEO accession GSE161553:

Go to https://www.ncbi.nlm.nih.gov/geo/query/acc.cgi?acc=GSE161553

Enter token onyfikkqpvmzjmd into the box

To review GEO accession GSE161551:

Go to https://www.ncbi.nlm.nih.gov/geo/query/acc.cgi?acc=GSE161551

Enter token szarkeskzbonzgh into the box

To review GEO accession GSE161544:

Go to https://www.ncbi.nlm.nih.gov/geo/query/acc.cgi?acc=GSE161544

Enter token klensayifzgppkl into the box

Competing interests

The authors declare that they have no competing interests.

Funding

This work was supported by the National Natural Science Foundation of China (81802375 to Shanshan Qin); the Faculty Development Grants from Hubei University of Medicine (2016QDJZR07 to Dandan Li, 2017QDJZR05 to Shanshan Qin, 2020QDJZR024 to Congcong Huang and 2020QDJZR012 to Pan Huang).

Authors' Contributions

QS conceived and designed the study. QS and LD wrote the paper. LD and SL performed most of the experiments. XM, ZX, HP, HC and CZ carried out initial data analyses and performed partial of the experiments. All authors contributed to drafting the manuscript. All authors read and approved the final manuscript.

Acknowledgements

We are very grateful to Dr. Jiwei Li and Dr. Zhaohui Ji (Lifegenes Biotechnology, Shanghai, China) for contributing to the RNA-Seq analysis. We are very grateful to Dr. Guoxi Huang (BioNanoSearching Biotechnology, Guangzhou, China) for contributing to RNA pulldown and RIP analysis.

References

1. Siegel RL, Miller KD, Fuchs HE, Jemal A. Cancer, Statistics. 2021. Ca-Cancer J Clin. 2021;71(1):7–33.
2. Sakai H, Kawakami H, Teramura T, Onodera Y, Somers E, Furuuchi K, et al. Folate receptor alpha increases chemotherapy resistance through stabilizing MDM2 in cooperation with PHB2 that is

overcome by MORAb-202 in gastric cancer. Clinical and Translational Medicine. 2021;11(6).
3. Wang XH, Jiang ZH, Yang HM, Zhang Y, Xu LH. Hypoxia-induced FOXO4/LDHA axis modulates gastric cancer cell glycolysis and progression. Clinical and Translational Medicine. 2021;11(1).
4. Wang J, Zhang M, Hu X, She J, Sun R, Qin S, et al. MiRNA-194 predicts favorable prognosis in gastric cancer and inhibits gastric cancer cell growth by targeting CCND1. FEBS Open Bio; 2021.
5. Fan HJ, Wang XX, Li WY, Shen MH, Wei Y, Zheng HQ, et al. ASB13 inhibits breast cancer metastasis through promoting SNAI2 degradation and relieving its transcriptional repression of YAP. Gene Dev. 2020;34(19–20):1359–72.
6. Li WY, Shen MH, Jiang YZ, Zhang RN, Zheng HQ, Wei Y, et al. Deubiquitinase USP20 promotes breast cancer metastasis by stabilizing SNAI2. Gene Dev. 2020;34(19–20):1310–5.
7. Du F, Li XW, Feng WB, Qiao CY, Chen J, Jiang MZ, et al. SOX13 promotes colorectal cancer metastasis by transactivating SNAI2 and c-MET. Oncogene. 2020;39(17):3522–40.
8. Li DD, Wang JJ, Zhang MX, Hu XH, She JJ, Qiu XM, et al. LncRNA MAGI2-AS3 Is Regulated by BRD4 and Promotes Gastric Cancer Progression via Maintaining ZEB1 Overexpression by Sponging miR-141/200a. Mol Ther-Nucl Acids. 2020;19:109–23.
9. Ye GW, Wang P, Xie ZY, Li JT, Zheng G, Liu WJ, et al. IRF2-mediated upregulation of lncRNA HHAS1 facilitates the osteogenic differentiation of bone marrow-derived mesenchymal stem cells by acting as a competing endogenous RNA. Clinical and Translational Medicine. 2021;11(6).
10. Davis MC, Kesthely CA, Franklin EA, MacLellan SR. The essential activities of the bacterial sigma factor. Can J Microbiol. 2017;63(2):89–99.
11. Li DD, She JJ, Hu XH, Zhang MX, Sun RN, Qin SS. The ELF3-regulated lncRNA UBE2CP3 is over-stabilized by RNA-RNA interactions and drives gastric cancer metastasis via miR-138-5p/ITGA2 axis. Oncogene. 2021.
12. Liu HT, Liu S, Liu L, Ma RR, Gao P. EGR1-Mediated Transcription of lncRNA-HNF1A-AS1 Promotes Cell-Cycle Progression in Gastric Cancer. Cancer Res. 2018;78(20):5877–90.
13. Li D, Cheng P, Wang J, Qiu X, Zhang X, Xu L, et al. IRF6 Is Directly Regulated by ZEB1 and ELF3, and Predicts a Favorable Prognosis in Gastric Cancer. Front Oncol. 2019;9:220.
14. Luo S, Lu JY, Liu L, Yin Y, Chen C, Han X, et al. Divergent lncRNAs Regulate Gene Expression and Lineage Differentiation in Pluripotent Cells. Cell Stem Cell. 2016;18(5):637–52.
15. Chen DD, Cheng JT, Chandoo A, Sun XW, Zhang L, Lu MD, et al. microRNA-33a prevents epithelial-mesenchymal transition, invasion, and metastasis of gastric cancer cells through the Snail/Slug pathway. Am J Physiol-Gastr L. 2019;317(2):G147-G60.
16. Yu L, Wu S, Che ST, Wu YZ, Han N. Inhibitory role of miR-203 in the angiogenesis of mice with pathological retinal neovascularization disease through downregulation of SNAI2. Cell Signal. 2020;71.
17. Ge XL, Li GY, Jiang L, Jia LQ, Zhang ZZ, Li XL, et al. Long noncoding RNA CAR10 promotes lung adenocarcinoma metastasis via miR-203/30/SNAI axis. Oncogene. 2019;38(16):3061–76.

18. Chen LL. Linking Long Noncoding RNA Localization and Function. Trends Biochem Sci. 2016;41(9):761–72.
19. Ali MM, Akhade VS, Kosalai ST, Subhash S, Statello L, Meryet-Figuiere M, et al. PAN-cancer analysis of S-phase enriched lncRNAs identifies oncogenic drivers and biomarkers. Nat Commun. 2018;9(1):883.
20. Satyanarayana A, Hilton MB, Kaldis P. p21 inhibits Cdk1 in the absence of Cdk2 to maintain the G1/S phase DNA damage checkpoint. Mol Biol Cell. 2008;19(1):65–77.
21. Fiaschi-Taesch NM, Salim F, Kleinberger J, Troxell R, Cozar-Castellano I, Selk K, et al. Induction of Human beta-Cell Proliferation and Engraftment Using a Single G1/S Regulatory Molecule, cdk6. Diabetes. 2010;59(8):1926–36.
22. Wen X, Liu X, Mao YP, Yang XJ, Wang YQ, Zhang PP, et al. Long non-coding RNA DANCR stabilizes HIF-1alpha and promotes metastasis by interacting with NF90/NF45 complex in nasopharyngeal carcinoma. Theranostics. 2018;8(20):5676–89.
23. Guan DY, Altan-Bonnet N, Parrott AM, Arrigo CJ, Li Q, Khaleduzzaman M, et al. Nuclear factor 45 (NF45) is a regulatory subunit of complexes with NF90/110 involved in mitotic control. Mol Cell Biol. 2008;28(14):4629–41.
24. Oh SC, Sohn BH, Cheong JH, Kim SB, Lee JE, Park KC, et al. Clinical and genomic landscape of gastric cancer with a mesenchymal phenotype. Nat Commun. 2018;9(1):1777.
25. Cristescu R, Lee J, Nebozhyn M, Kim KM, Ting JC, Wong SS, et al. Molecular analysis of gastric cancer identifies subtypes associated with distinct clinical outcomes. Nat Med. 2015;21(5):449–56.
26. Wang YF, Shi J, Chai KQ, Ying XH, Zhou BHP. The Role of Snail in EMT and Tumorigenesis. Curr Cancer Drug Tar. 2013;13(9):963–72.
27. Jayachandran A, Konigshoff M, Yu H, Rupniewska E, Hecker M, Klepetko W, et al. SNAI transcription factors mediate epithelial-mesenchymal transition in lung fibrosis. Thorax. 2009;64(12):1053–61.
28. Nieto MA, Huang RYJ, Jackson RA, Thiery JP. Emt: 2016 Cell. 2016;166(1):21–45.
29. Zheng H, Kang Y. Multilayer control of the EMT master regulators. Oncogene. 2014;33(14):1755–63.
30. Bryzghalov O, Szczesniak MW, Makalowska I. Retroposition as a source of antisense long non-coding RNAs with possible regulatory functions. Acta Biochim Pol. 2016;63(4):825–33.
31. Jadaliha M, Gholamalamdari O, Tang W, Zhang Y, Petracovici A, Hao Q, et al. A natural antisense lncRNA controls breast cancer progression by promoting tumor suppressor gene mRNA stability. PLoS Genet. 2018;14(11):e1007802.

Figures

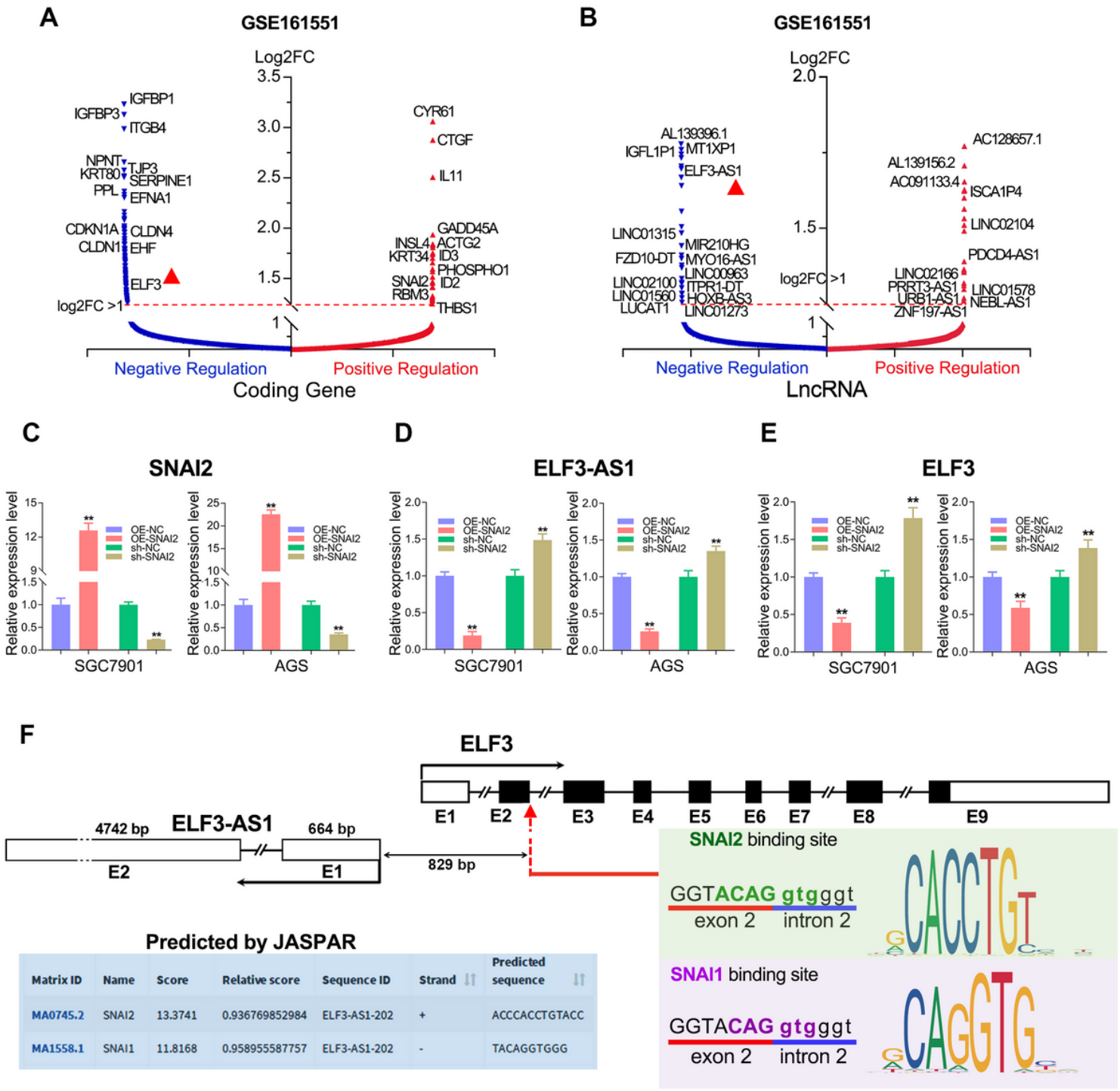

Figure 1

Identification of the SNAI2-regulated lncRNAs in GC by RNA-seq. (A, B) The protein-coding genes and the lncRNAs that positively (Red) or negatively (Blue) regulated by SNAI2 were shown in volcano plots (log2FC>1). (C) The overexpression and knockdown efficiency of SNAI2 in the SGC7901 and AGS cell lines were verified by qRT-PCR. (D, E) The ELF3-AS1 and ELF3 expression were detected after overexpression/knockdown of SNAI2 in GC cell lines. (F) The promoter analysis by JASPAR web tool

revealed SNAI2 and SNAI1 could bind on the common promoter of lncRNA ELF3-AS1 and ELF3. **, P < 0.01.

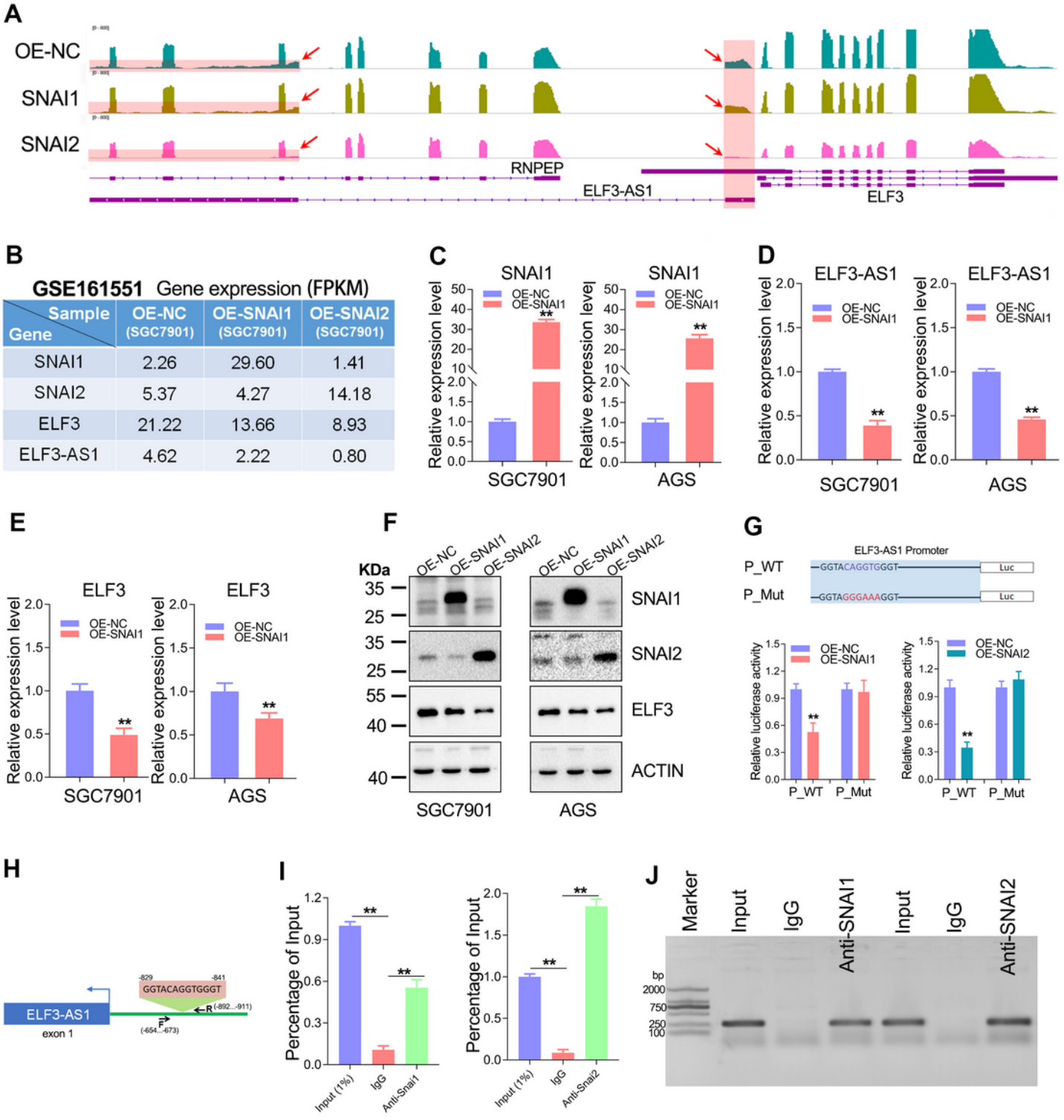

Gene \ Sample	OE-NC (SGC7901)	OE-SNAI1 (SGC7901)	OE-SNAI2 (SGC7901)
SNAI1	2.26	29.60	1.41
SNAI2	5.37	4.27	14.18
ELF3	21.22	13.66	8.93
ELF3-AS1	4.62	2.22	0.80

Figure 2

ELF3-AS1 and ELF3 are transcriptionally inhibited by both SNAI2 and SNAI1 in GC. (A) The transcripts abundance of ELF3-AS1 and ELF3 in SNAI2/SNAI1 overexpression cell lines was detected by RNA-seq. (B) The normalized expression (FPKM value) of SNAI1, SNAI2, ELF3 and ELF3-AS1 were shown in the

plot. (C) The overexpression efficiency of SNAI1 in GC cell lines was verified by qRT-PCR. (D, E) The ELF3-AS1 and ELF3 expression were detected after overexpression of SNAI1. (F) Overexpression of SNAI1 or SNAI2 significantly decreased the protein level of ELF3. (G) Dual-luciferase reporter assay showed that the predictive binding site of SNAI1 or SNAI2 is necessary for their inhibition on Luc expression. (H) Diagram showing the primers location used in CHIP-qPCR/PCR. (I, J) Chip assay showed that both SNAI1 and SNAI2 could bind to the promoter of ELF3 or ELF3-AS1. **, P < 0.01.

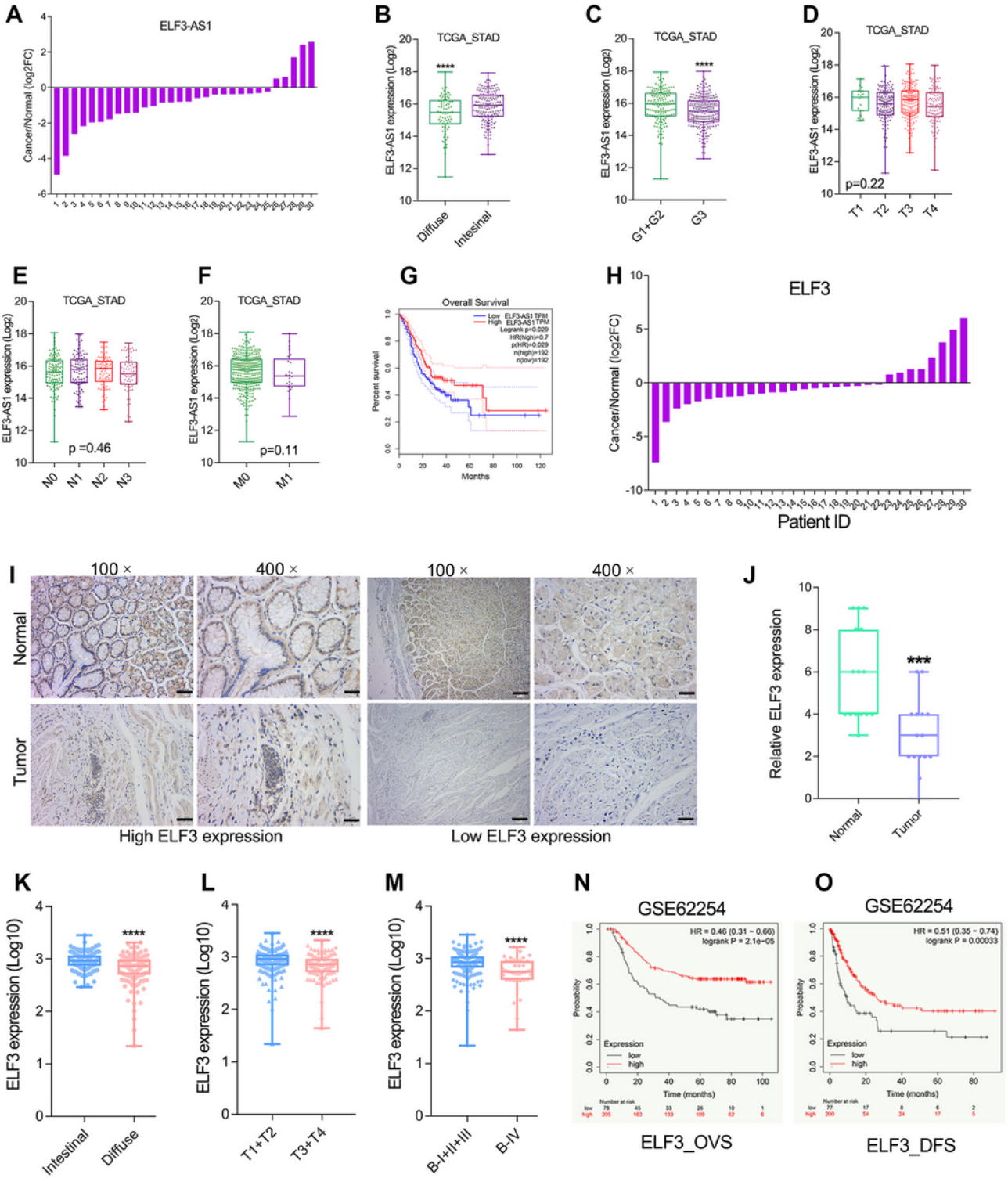

Figure 3

Reduced expression of ELF3-AS1 and ELF3 correlates with poor prognosis in GC. (A) The ELF3-AS1 expression in 30 paired of GC tissues and adjacent non-tumor tissues was examined by qRT-PCR. (B, C) The ELF3-AS1 expression in GC patients with different histopathological types and differentiation degree. (D-F) The ELF3-AS1 expression in GC patients with different TNM stages. (G) Overall Survival analysis using GEPIA webtool showed that ELF3-AS1 predicts favorable prognosis in GC. (H) The ELF3 expression level in 30 paired of GC tissues and adjacent non-tumor tissues was examined by qRT-PCR. (I) Representative IHC images on the tissue microarray (TMA) probed with the anti-ELF3 antibody (scale bars=100 μm or 25 μm, respectively) are shown. (J) IHC analysis of ELF3 expression in 15 cases of GC tissues and paired normal tissues. (K) Difference in expression levels of ELF3 between intestinal GC tissues and diffuse GC tissues. (L, M) ELF3 expression level in different T-stages and Borrmann-stages of GC tissues from GSE62254 cohort. (N, O) Kaplan-Meier survival curves of overall survival and disease-free survival based on ELF3 expression in the GC cohort GSE62254. **, $P < 0.01$. ***, $P < 0.001$. ****, $P < 0.0001$.

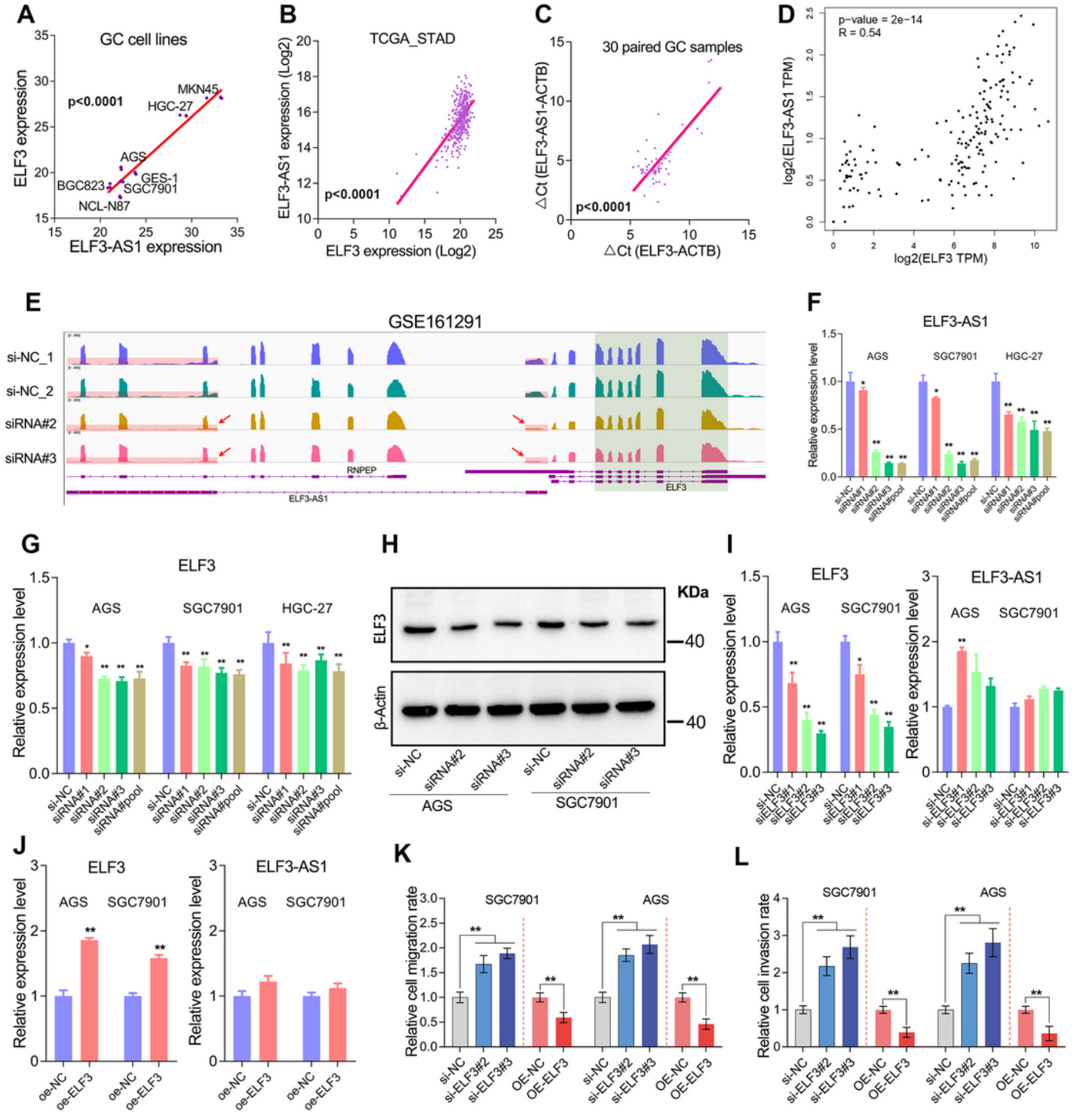

Figure 4

ELF3 negatively regulates cell metastasis but cannot regulate ELF3-AS1 expression in GC. (A-C) ELF3-AS1 and ELF3 were highly co-expressed in GC cell lines and tissues. (D) ELF3-AS1 and ELF3 were highly co-expressed in normal stomach tissues. (E) The transcripts abundance of ELF3-AS1 and ELF3 was detected by RNA-seq in ELF3-AS1-depleted cell lines. (F) The knockdown efficiency of ELF3-AS1 in GC cell lines was verified. (G, H) Knockdown of ELF3-AS1 decreased the mRNA and protein level of ELF3 in GC. (I,

J) The ELF3 knockdown/overexpression had no obvious effect on ELF3-AS1 expression. (K, L) ELF3 negatively regulates the migration and invasion of GC cells. **, P < 0.01.

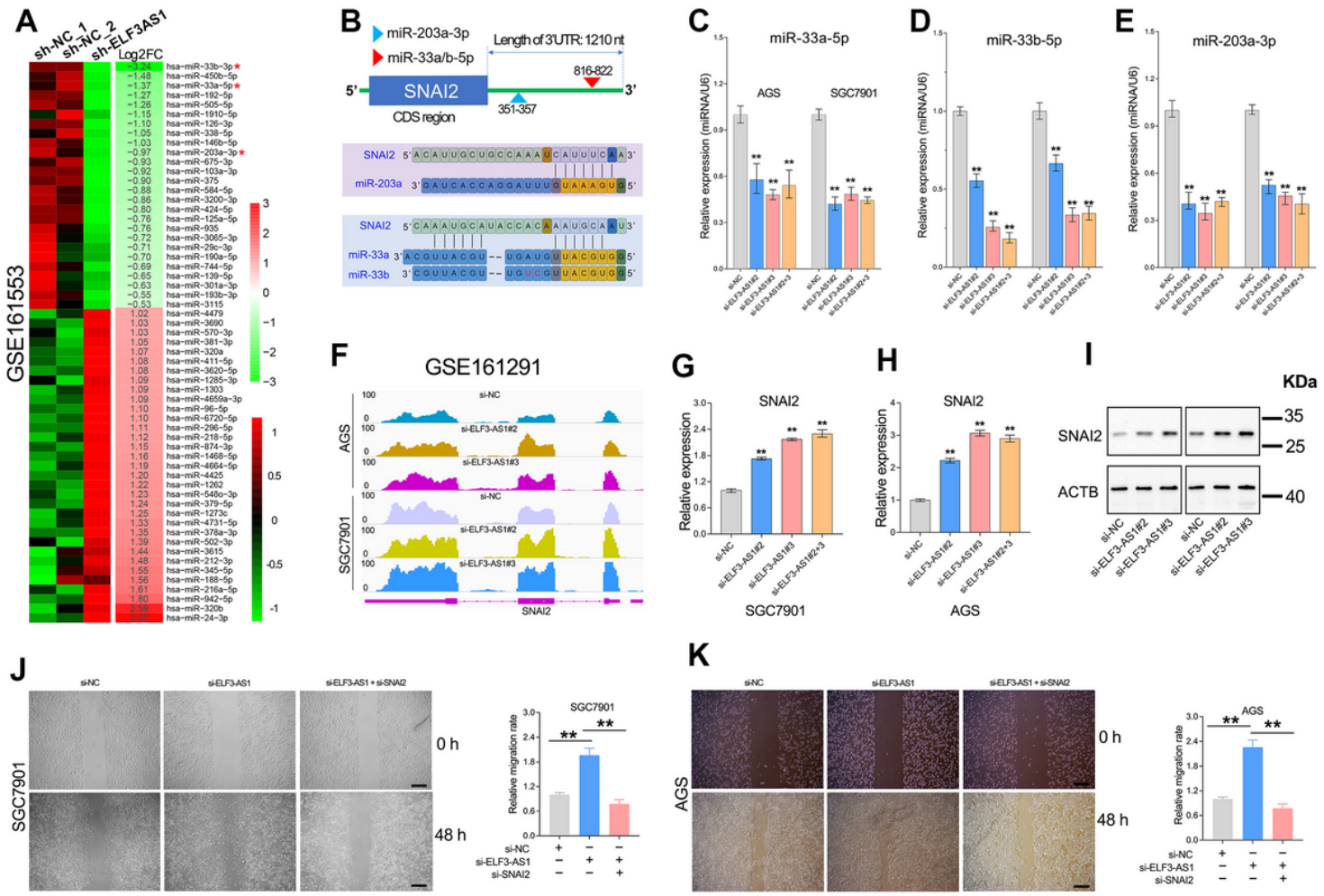

Figure 5

ELF3-AS1 mainly inhibits GC metastasis through repressing SNAI2 signaling. (A) The heat map reveals the differential expressed miRNAs altered by ELF3-AS1 knockdown (left panel), and the log2FC values (ELF3-AS1/NC) were shown in the right panel. The red asterisk indicates the miRNAs targeting SNAI2. (B) The binding sites of miR-33a/b and miR-203a on 3'UTR of SNAI2 were predicted by TargetScan web tool. (C-E) The expression level of miR-33a, miR-33b and miR-203a were detected in the ELF3-AS1 knockdown cell lines. (F) The transcripts abundance of SNAI2 in ELF3-AS1 knockdown cell lines. (G-I) The mRNA and protein level of SNAI2 were determined in the ELF3-AS1-depleted GC cell lines. (J, K) Rescue assay in two GC cell lines both confirmed that ELF3-AS1 inhibited GC metastasis through SNAI2 signaling. Scale bars=50μm **P < 0.01.

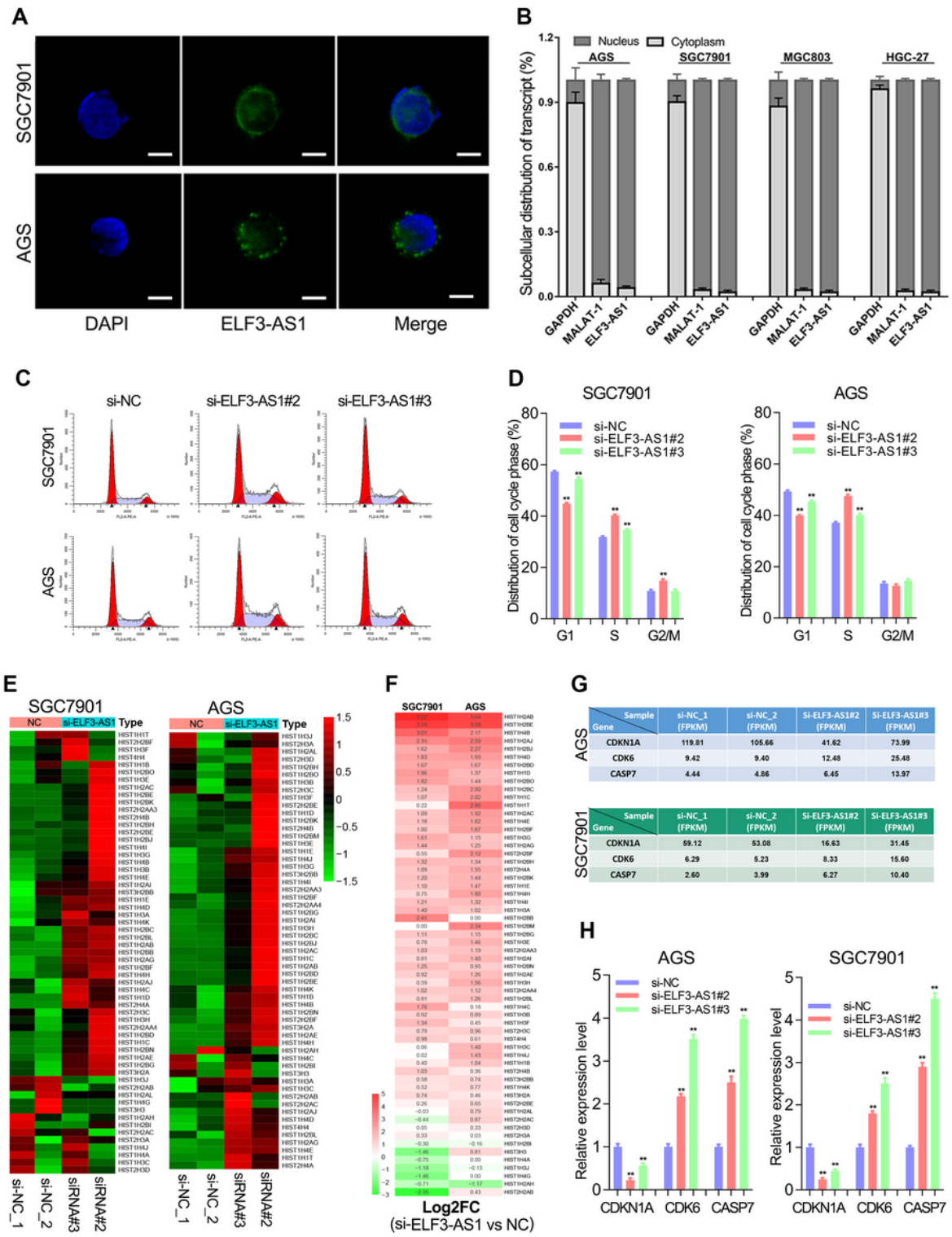

Figure 6

Nuclear-localized lncRNA ELF3-AS1 regulates cell cycle progression by affecting G1/S transition and histone synthesis. (A) Subcellular localization of ELF3-AS1 by RNA FISH in GC cell lines. Bar, 10 μm. (B) The ELF3-AS1 transcripts were mainly located in the nucleus of GC cell lines. (C, D) ELF3-AS1 negatively regulated the G1/S transition of the cell cycle in GC. (E, F) The histone-coding genes significantly regulated by ELF3-AS1 knockdown (|Log2FC|>0.7) were shown in the heat map. Almost all the histone-

coding genes were upregulated in the ELF3-AS1-depleted cell lines. (G) The normalized expression (FPKM value) of CDKN1A, CDK6 and CASP7 after knockdown of ELF3-AS1 in GC cell lines. (H) The mRNA level of CDKN1A, CDK6 and CASP7 were determined after knockdown of ELF3-AS1. **P < 0.01.

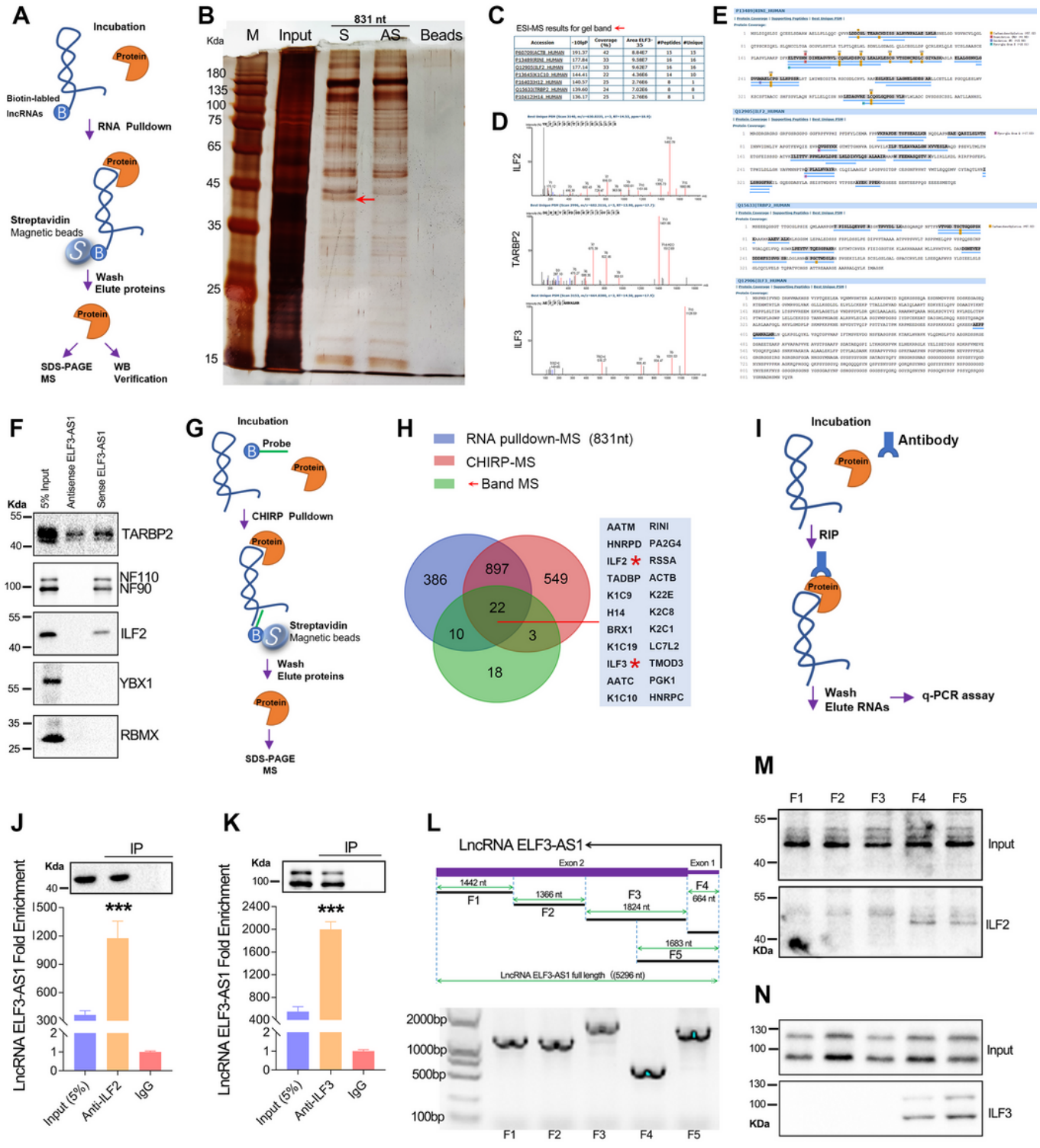

Figure 7

ELF3-AS1 directly interacts with the ILF2/ILF3 protein complex. (A) Schematic workflow of the RNA pull-down assay for identification of ELF3-AS1 binding proteins. The sense (S) and anti-sense (AS) of ELF3-

AS1 RNA were biotinylated, refolded, and incubated with SGC7901 cell lysates. (B-E) Identification of ELF3-AS1 binding proteins using a combined RNA pulldown-MS assay. According to the MS analysis of band labeled with a red arrow, RINI, TARBP2, ILF2 and ILF3 were most possible RNA binding proteins interacted with ELF3-AS1. (F) Validation of ELF3-AS1 binding proteins that obtained by RNA pulldown using western blotting. (G) Schematic workflow of the CHIRP assay for identification of ELF3-AS1 binding proteins. (H) The Venn plot of the ELF3-AS1 binding proteins identified by three mass spectrometry. (I) Schematic workflow of the RNA immunoprecipitation (RIP) for verification of ELF3-AS1 binding proteins. (J, K) RIP-qPCR assay verified the interaction between ELF3-AS1 and ILF2/ILF3. Fold Enrichment was determined relative to an IgG control. (L) Schematic of the truncated fragments of lncRNA ELF3-AS1. (M, N) Western blot was used to verify the ILF2 and ILF3 proteins in the pellets pulled down by ELF3-AS1 RNA fragments of different lengths. **, $P < 0.01$.

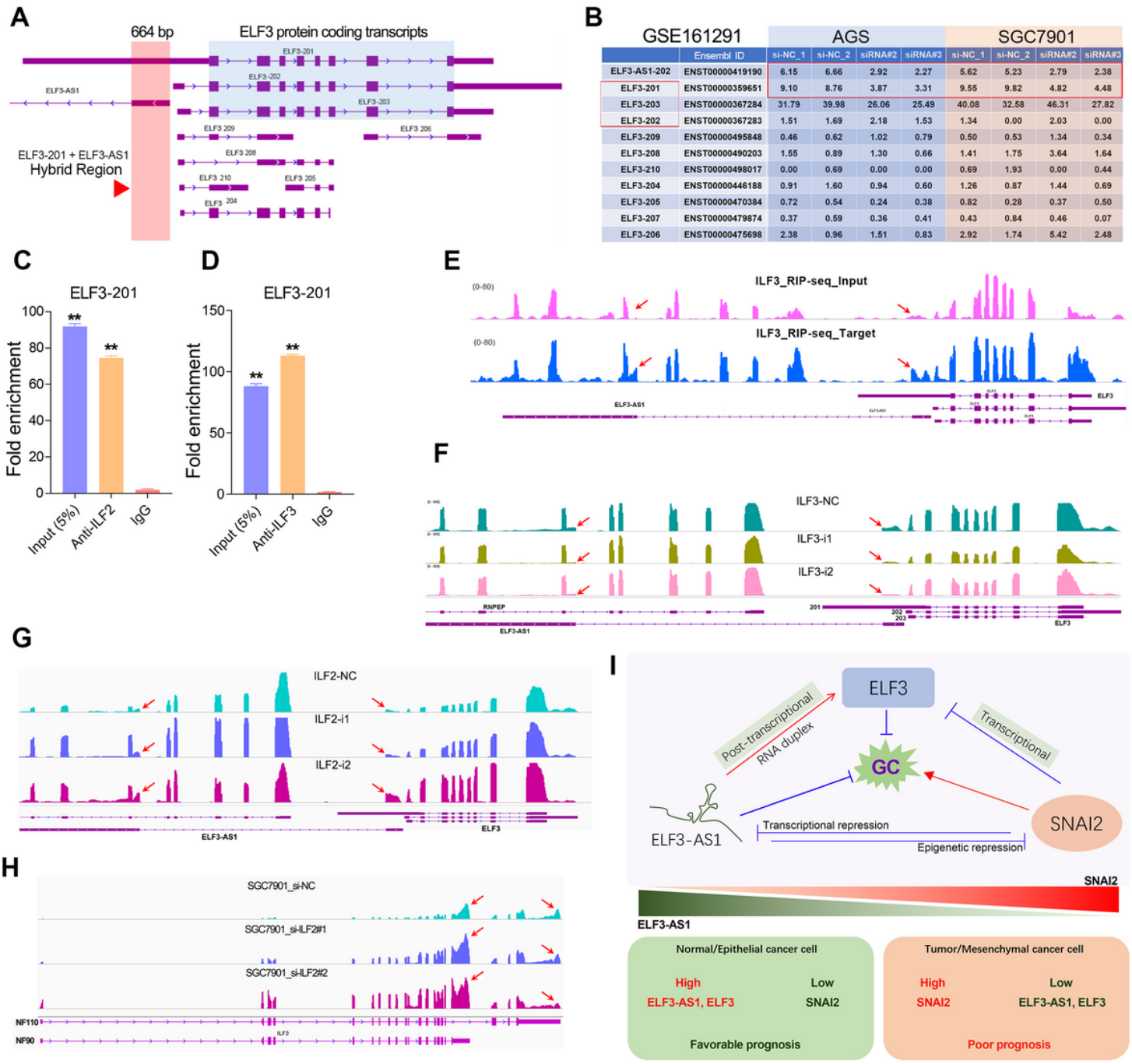

	Ensembl ID	AGS si-NC_1	AGS si-NC_2	AGS siRNA#2	AGS siRNA#3	SGC7901 si-NC_1	SGC7901 si-NC_2	SGC7901 siRNA#2	SGC7901 siRNA#3
ELF3-AS1-202	ENST00000419190	6.15	6.66	2.92	2.27	5.62	5.23	2.79	2.38
ELF3-201	ENST00000359651	9.10	8.76	3.87	3.31	9.55	9.82	4.82	4.48
ELF3-203	ENST00000367284	31.79	39.98	26.06	25.49	40.08	32.58	46.31	27.82
ELF3-202	ENST00000367283	1.51	1.69	2.18	1.53	1.34	0.00	2.03	0.00
ELF3-209	ENST00000495848	0.46	0.62	1.02	0.79	0.50	0.53	1.34	0.34
ELF3-208	ENST00000490203	1.55	0.89	1.30	0.66	1.41	1.75	3.64	1.64
ELF3-210	ENST00000498017	0.00	0.69	0.00	0.00	0.69	1.93	0.00	0.44
ELF3-204	ENST00000446188	0.91	1.60	0.94	0.60	1.26	0.87	1.44	0.69
ELF3-205	ENST00000470384	0.72	0.54	0.24	0.38	0.82	0.28	0.37	0.50
ELF3-207	ENST00000479874	0.37	0.59	0.36	0.41	0.43	0.84	0.46	0.07
ELF3-206	ENST00000475698	2.38	0.96	1.51	0.83	2.92	1.74	5.42	2.48

Figure 8

The ILF2/ILF3 interacts with ELF3-AS1/ELF3 RNA duplex to affect RNA duplex stability. (A) The gene structure and location of ELF3-AS1 and ELF3 genes. (B) The normalized expression (FPKM value) of different ELF3 transcripts after knockdown of ELF3-AS1 was shown in the plot. Knockdown of ELF3-AS1 remarkably decreased the expression of ELF3-201 transcripts in GC cell lines. (C, D) RIP-qPCR assay verified the interaction between ELF3-201 transcripts and ILF2/ILF3 complex. (E) The transcripts abundance of ELF3 and ELF3-AS1 detected by RIP-seq_anti-ILF3 (GSE163815) was shown in the plot. (F) The transcripts abundance of ELF3 and ELF3-AS1 in ILF3-silenced samples was detected by RNA-seq. (G) The transcripts abundance of ELF3 and ELF3-AS1 in ILF2-silenced samples was detected by RNA-seq. (H)

ILF2 knockdown affected the alternative splicing of ILF3 gene. (I) The working model of the SNAI2-ELF3-AS1 feedback loop. **, P < 0.01.

Supplementary Files

This is a list of supplementary files associated with this preprint. Click to download.

- GraphicalAbstract.png
- AdditionalFile1.docx
- AdditionalFile2.docx
- TableS3.xlsx
- TableS4.xlsx
- TableS5.xlsx
- TableS6.xlsx